J Nanopart Res (2011) 13:6439–6445
DOI 10.1007/s11051-011-0397-9

RESEARCH PAPER

Gold nanoparticles produced in a microalga

Tiyaporn Luangpipat · Isabel R. Beattie · Yusuf Chisti · Richard G. Haverkamp

Received: 27 May 2010 / Accepted: 26 April 2011 / Published online: 11 May 2011

Abstract An efficient biological route to production of gold nanoparticles which allows the nanoparticles to be easily recovered remains elusive. Live cells of the green microalga *Chlorella vulgaris* were incubated with a solution of gold chloride and harvested by centrifugation. Nanoparticles inside intact cells were identified by transmission electron microscopy and confirmed to be metallic gold by synchrotron based X-ray powder diffraction and X-ray absorption spectroscopy. These intracellular gold nanoparticles were 40–60 nm in diameter. At a concentration of 1.4% Au in the alga, a better than 97% recovery of the gold from solution was achieved. A maximum of 4.2% Au in the alga was obtained. Exposure of *C. vulgaris* to solutions containing dissolved salts of palladium, ruthenium, and rhodium also resulted in the production of the corresponding nanoparticles within the cells. These were surmised to be also metallic, but were produced at a much lower intracellular concentration than achieved with gold. Iridium was apparently toxic to the alga. No nanoparticles were observed using platinum solutions. *C. vulgaris* provides a possible route to large scale production of gold nanoparticles.

T. Luangpipat · I. R. Beattie · Y. Chisti · R. G. Haverkamp (✉)
School of Engineering and Advanced Technology, Massey University, Palmerston North 4442, New Zealand
e-mail: r.haverkamp@massey.ac.nz

Keywords Nanoparticles · *Chlorella vulgaris* · Gold · Platinum · Palladium · Iridium · Ruthenium · Rhodium · Nanobiotechnology

Introduction

Metal nanoparticles are attracting attention for applications in catalysis, drug delivery, photonics and other areas (Haverkamp 2010). For use in catalysis the particles must be small so that a large catalytically active surface is presented by a limited amount of expensive material. Attaining a small particle size is especially important for gold, as it becomes reactive only when the particle size is of the order of a few nanometres (Haruta 2003). A small size is important, but the surface must also have a small radius of curvature as this influences surface chemistry and, therefore, the catalytic properties. Nanoparticles with angular shapes are preferable as they have a generally higher proportion of the regions with small radii of curvature compared to spherical particles of the same volume.

Chemical methods are conventionally used to produce nanoparticles. Compared to these methods, biological systems potentially offer a greener route to production. Nanoparticles of gold (Anderson et al. 1998; Gardea-Torresdey et al. 2002; Sharma et al. 2007), silver (Haverkamp and Marshall 2009), copper (Manceau et al. 2008), and a gold–silver–copper alloy (Haverkamp et al. 2007) have been produced in live

vascular plants. Although higher plants have been commonly used to make nanoparticles, no processes appear to exist for recovering the particles from them (Lamb et al. 2001; Marshall et al. 2007). Plant matter can of course be harvested, ground and digested, but releasing the particles from within the cells has proved difficult. Alternatively, dried plant biomass may be burnt to recover the metal particles, but this has the potential to damage them through unwanted fusing and loss of angularity.

The cyanobacteria *Anabaena*, *Calothrix* and *Leptolyngbya* have been shown to form gold, silver, palladium and platinum nanoparticles intracellularly (Brayner et al. 2007). Fungi and heterotrophic bacteria have also been shown to form gold and silver nanoparticles (Mohanpuria et al. 2008; Reith et al. 2009). Nanometal particles do not appear to have been produced in live algal cells, although cell-free extracts of the microalga *C. vulgaris* have been used to produce gold nanoplates (Xie et al. 2007). Here the authors demonstrate the intracellular production of gold and other metal nanoparticles in the microalga *C. vulgaris*.

In a biological system, nanoparticles are formed by reduction of the metal ion absorbed as a soluble salt. The reduction potential and capacity of the system therefore determine its effectiveness as a production vehicle for nanoparticles. The reduction potential within higher plants is around 0 V (with respect to the standard hydrogen electrode) and consequently salts of only the precious and semiprecious metals can be converted to nanoparticles (Haverkamp and Marshall 2009). Metals such as platinum, palladium, ruthenium, rhodium and iridium meet the requisite criteria but have not been shown to form nanoparticles in live plants.

Microalgae are primitive microscopic plants. Compared to higher plants, microalgae have important advantages as cell factories for producing nanoparticles. Unlike higher plants, microalgae grow extremely rapidly. For example, microalgae double their mass on average ten-times faster than higher plants (Chisti 2010). Methods are well-developed for large scale culture of microalgae under controlled conditions (Chisti 2007; Chisti 2008) to produce a consistent supply of the biomass. In addition, aqueous slurries of microalgae cells are easily handled in large scale production processes. Algal broths are easy to pump and homogenously mix with solutions of metal salts. Algal biomass can be harvested (Molina Grima et al. 2003) and the cells can be readily disrupted (Chisti and Moo-Young 1986) using commercial processing equipment to release the intracellular nanoparticles.

Chlorella vulgaris was selected for this study as it grows rapidly and is a well-established commercial alga. *C. vulgaris* tolerates a wide range of salinities. This is important in producing nanoparticles as live algal cells must be exposed to a metal salt solution that is relatively concentrated to ensure rapid generation of a large quantity of nanoparticles.

Materials and methods

Chlorella vulgaris was grown photoautotrophically to a concentration of around 2 g/L in BG11 culture medium (Andersen 2005) formulated with filter sterilized "seawater". The latter was made by dissolving natural unrefined Southern Pacific Ocean salt (40 g/L; Pacific Natural Fine Salt, Dominion Salt Ltd, Marlborough, New Zealand) in potable tap water. The algal broth was diluted 1:1 by volume with this autoclaved (121 °C, 15 min) and cooled BG11 seawater medium. The alga was allowed to grow for a further 48 h in 250 mL Erlenmeyer flasks held at 25 °C under illumination (10 μE m^{-2} s^{-1}) in an agitated (100 rpm) incubator. Metal salt solutions (0.2 g metal/L, 10 mL) that had been separately autoclaved (121 °C, 15 min) and cooled to room temperature were then aseptically added to the different 100 mL samples of the algal broth. Solutions of the following salts were used, each in a separate experiment: $HAuCl_4 \cdot 3H_2O$, $H_2PtCl_6 \cdot 6H_2O$, $PdCl_2$, $IrCl_4$ and $RhCl_3$. In a control treatment, 10 mL of deionized water was added to the algal broth instead of a metal salt solution. All chemicals had been purchased from Artcraft Chemicals Ltd (Altamont, NY, USA), unless specified otherwise.

The algal broth samples that had been mixed with the metal salt solutions and the control sample were further incubated for 48 h as specified above. Subsequently, the algal biomass from each flask was harvested by centrifugation (at a force of 4,150 g, 10 min) and washed five times with deionized water. Each wash involved resuspending the biomass in 100 mL of deionized water and recovery by centrifugation as above. A sample of the biomass paste

recovered after the final wash was used directly for transmission electron microscopy (TEM). The remainder of the paste was freeze dried and ground with a mortar and pestle for powder diffraction and XAS analyses.

In addition, the rate of uptake of gold by the alga was examined and a mass balance on the uptake process was carried out in a separate series of experiments. These involved 3, 12 and 48 h of exposure of the cells to $HAuCl_4$ solutions. The filtrate from the three successive washes for each of the above exposure periods was collected and pooled in separate containers. The gold uptake studies were performed on larger samples (1 L) of the broth containing 1.4–1.6 g/L biomass and exposed to 100 mL of a solution containing Au at a concentration of 0.02 g Au/L.

For transmission electron microscopy (TEM) algal samples were fixed with 3% glutaraldehyde, 2% formaldehyde and 0.1 M phosphate buffer at pH 7.2. There was no secondary fixing with osmium. This was followed by a buffer wash, acetone series dehydration and setting in Procure 812 epoxy resin. TEM sections were cut on a diamond knife, mounted on copper grids and imaged without staining. A Philips CM10 TEM (Philips, Eindhoven, The Netherlands) was used with an acceleration voltage of 60 kV. Images were recorded with a SIS Morada high-resolution camera (Olympus Soft Imaging Solutions GmbH, Münster, Germany).

Total scattering X-ray spectra were recorded using the powder diffraction beamline at the Australian Synchrotron (Haverkamp and Wallwork 2009), Melbourne, Australia. The beamline used a Mythen II massively parallel silicon microstrip detector. Samples were packed in 0.3 mm boron-rich glass capillaries with 0.01 mm wall thickness (W. Müller, Schönwalde, Germany). Packing densities were measured and ranged from 25 to 35%. The scattering pattern was measured at angles ranging from 4° to 149°. The X-ray wavelength was 0.59074(1) Å (21 keV) and the acquisition time was 900 s. Measurements were made on an empty capillary and the vacant beam X-ray path for background corrections. Data processing to obtain the pair distribution function (PDF) information used the freely available software PDFGetX2 (Qiu et al. 2004). The observed PDFs were modelled using the software PDFgui (Farrow et al. 2007), also freely available.

X-ray absorption spectra were recorded on the XAS beamline at the Australian synchrotron, Melbourne, Australia. Au L3 edge absorption spectra were recorded in transmission mode using a set of flow-through ion chambers filled with He. Energy steps of 2.5 eV were employed near the edge with counting for 0.2 s per step. Energy resolution was about 1.8 eV. The energy scale was calibrated by simultaneously measuring a Au foil placed between the two downstream containers. The photon flux was in the range 10^{11}–10^{12} photons s^{-1}. Multiple scans were performed and summed (after checking for changes due to beam damage). Samples for XAS were packed in 5 mm thick sample holders. Reference standards were 5 μm Au foil, 10% $Au(OH)_3$ diluted in boron nitride, 10% $HAuCl_4$ in boron nitride, both in 1 mm thick sample holders. The X-ray beam was about 1.5 × 0.4 mm at the sample.

Analysis for gold in the dried alga and the filtrate was carried out by SGS Minerals Laboratory, Waihi, New Zealand. Algal samples were analyzed by fire assay by fusion with lead at 1080 °C then cupelled to remove the lead. The remaining prill was digested in nitric and hydrochloric acid and diluted. These solutions and the filtrate solutions were aspirated into a Varian 50B Atomic Absorption Spectrometer and read with a gold lamp at 242.8 nm.

Results and discussion

Almost all (97.0–98.4%) of the gold added to the algal broth was taken up by the cells within the first 3 h in the larger scale experiments. Gold uptake did not significantly increase with a longer exposure to gold solutions. This suggests that gold is firmly absorbed by the cells, or incorporated within them, and does not readily wash out. The gold concentration in the freeze-dried algal material was 1.4% Au for samples taken at all time intervals. The shortest exposure period used was 3 h, but a shorter period may be sufficient to fully capture the gold. The smaller scale uptake experiments with a larger ratio of gold to biomass resulted in a concentration of 4.2% Au in the algae.

Algal cells were found to be intact after exposure to the gold solutions for up to 48 h. The cells contained gold nanoparticles throughout the cytoplasm (Fig. 1), but generally not within the organelles

and starch granules. This suggests that the gold ions had sufficient time to diffuse throughout the cell before being reduced to metal. The number of gold nanoparticles contained within each cell was high, although variable. Most cells contained the nanoparticles.

The gold nanoparticles in the cytoplasm ranged in equivalent diameter from 10 to 200 nm, but most were in the 40–60 nm diameter range (Fig. 1). The particles were mostly spheroidal or polyhedral in shape with an aspect ratio less than 2, but some rod-shaped particles existed (Fig. 1b). A close inspection of Fig. 1b reveals the presence of many extremely fine nanoparticles ($\sim$3 nm in diameter) embedded within the wall of the algal cell. These particles were observed also in the control samples and, therefore, are not likely to be gold.

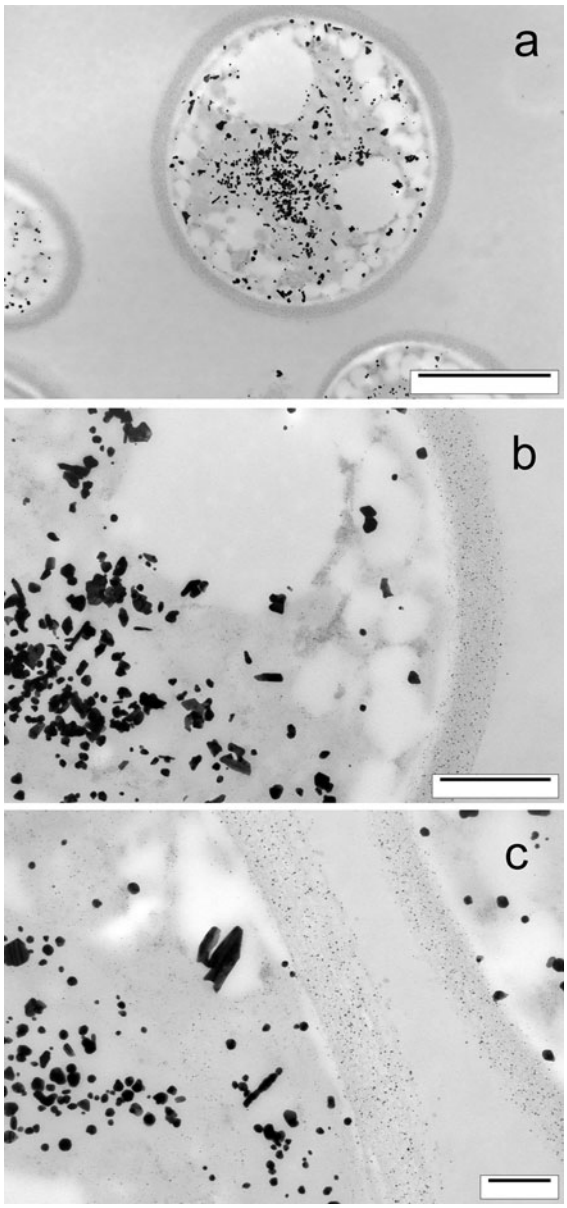

Fig. 1 Gold nanoparticles in algal cells. TEM images of *C. vulgaris* cells with gold nanoparticles. *Scale bars* **a** 2000 nm. **b** 500 nm. **c** 200 nm

X-ray scattering of the freeze dried sample showed Bragg peaks due to the presence of nanocrystalline gold. The total scattering spectrum was analyzed with a pair distribution function and fitted well to the

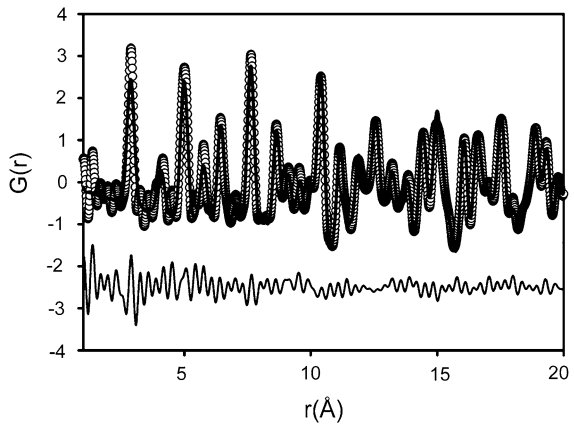

Fig. 2 Pair distribution function of X-ray scattering for gold nanoparticles in *C. vulgaris*. *Circles*, PDF from recorded scattering; *upper solid line*, fitted model for gold metal; *lower solid line*, difference between the recorded PDF and the fitted model

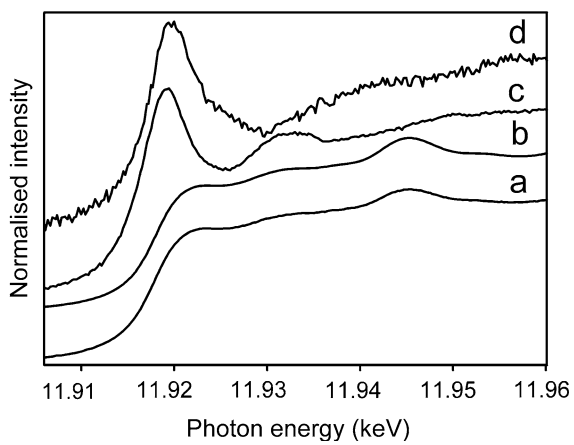

Fig. 3 XANES spectra of **a** Au foil. **b** *C. vulgaris* containing Au nanoparticles. **c** $HAuCl_4$. **d** $Au(OH)_3$

crystallographic data for gold metal (Suh et al. 1988) (Fig. 2). The best fit gave a crystallite size of 75 nm which was consistent with the size observed by TEM.

The Au L_3 XANES of the alga containing gold nanoparticles (Fig. 3a) showed a spectrum that was almost identical to the spectrum of the gold foil (Fig. 3b). The spectra of Au(III) containing compounds $HAuCl_4$ and $Au(OH)_3$ (Fig. 3c, d) in comparison exhibit a marked white line feature near the absorption edge, which was not exhibited by the Au(0) materials. Possible alteration of the samples by the X-ray analysis beam was investigated for all samples, particularly the possibility of the reduction of Au(III). $HAuCl_4$ was found to be remarkably stable under the X-ray flux present in during the XANES analysis with no significant degradation observed after 90 min of exposure. $Au(OH)_3$ was less stable with a gradual reduction of the white line feature of the spectrum during X-ray exposure, amounting to about 50% reduction after 30 min. The acquisition of the first XANES spectrum (as shown in Fig. 3d) was completed within 8 min of exposure to the X-ray beam. Likewise XANES spectra of the algal samples were recorded within about 8 min of initial exposure to the X-ray beam. Therefore, little X-ray reduction of gold was likely to have occurred during the measurements and the recorded spectrum reflected the original composition of the material. The XANES therefore clearly identified the gold nanoparticles within the alga as consisting of Au(0).

Although *C. vulgaris* readily reduced Au^{3+} to metallic gold, it was less effective in producing metal nanoparticles of the other noble metals.

Cells that had been exposed to palladium contained localized regions of particles within the

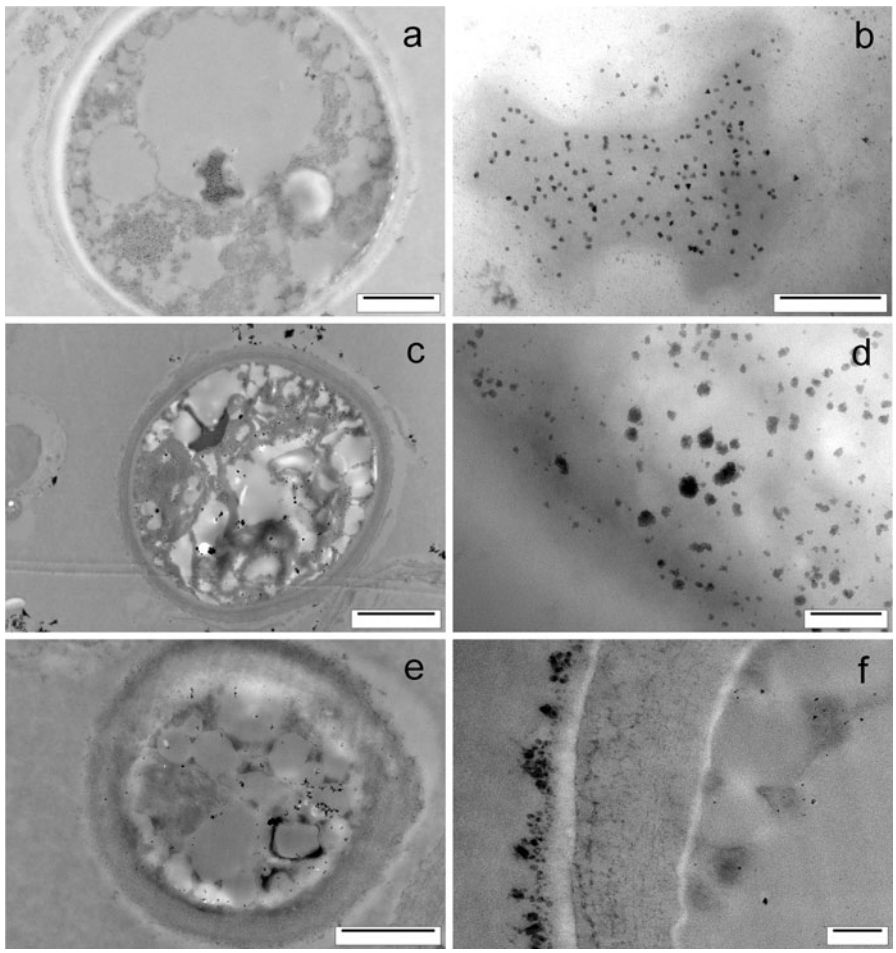

Fig. 4 Pd, Ru and Rh nanoparticles in and around *C. vulgaris* cells. **a** Pd deposits inside an algal cell. **b** Enlargement of Pd nanoparticles in an algal cell. **c** Ru deposits in and around an algal cell. **d** Enlargement of Ru nanoparticles in an algal cell. **e** Rh deposits in and around an alga cell. **f** Enlargement of Rh nanoparticles in and around an alga cell. *Scale bars* **c** 2000 nm; **a** and **e** 1000 nm; **b**, **d** and **f** 200 nm

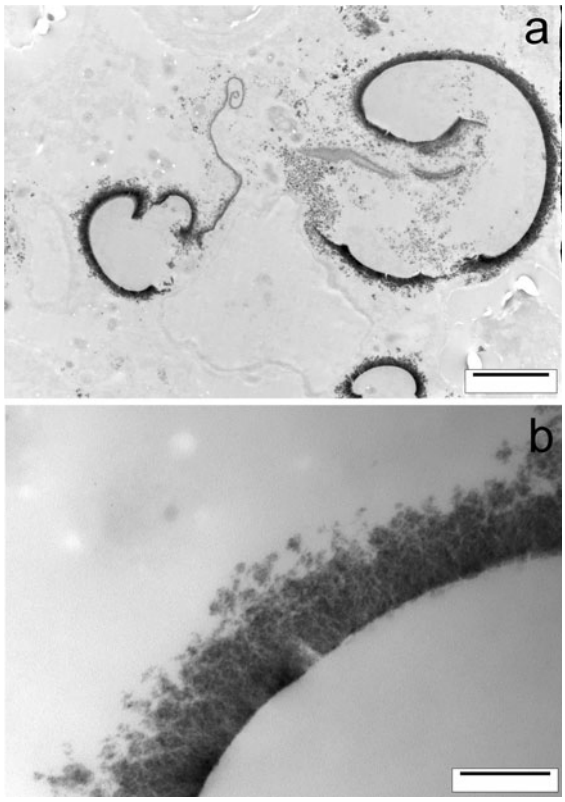

Fig. 5 Precipitate around *C. vulgaris* cell walls presumed to be metallic iridium. **a** Ir precipitate around the outside of disrupted algal cells, *scale bar* 2000 nm. **b** Enlargement of an Ir precipitate on a cell wall, *scale bar* 200 nm

cytoplasm (Fig. 4a, b). The particles in these regions were 5–12 nm in diameter and all had angular shapes appearing as triangles, squares and hexagons in a projection of the cell. The intracellular concentration of these particles was low compared to the observations with gold.

For ruthenium, some clumps of particles were seen both inside and outside the cells (Fig. 4c, d), but the particles in these clumps did not appear to be highly crystalline. Similarly with rhodium, some particles were formed both inside and outside the cells (Fig. 4e, f). A large number of particles were deposited as a layer on the outside of the cell wall (Fig. 4f). This was likely because most of the rhodium ions were precipitated or reduced on contact with the organic molecules of the cell wall and therefore did not transport into the cells. Cells that had been exposed to iridium had mostly lysed by 48 h (Fig. 5), suggesting that iridium were toxic to the alga. A precipitate of what is presumed to be an iridium compound was clearly seen on the outside of the broken cell envelope (Fig. 5b). No nanoparticles or precipitates were observed with platinum.

In contrast to the gold treated cells, no crystalline phases were detected by powder X-ray diffraction in cells that had been exposed to the other noble metal ions. Either the concentration of the metal precipitate was too low to be detected, or the deposited material was not sufficiently crystalline.

Although the presence of elemental particles of the noble metals other than Au could not be conclusively established in *C. vulgaris*, the reduction potentials for these metals suggest that they are in principle capable of being reduced in living systems such as plants (Haverkamp and Marshall 2009) so long as they can be transported across the cell wall. This does not appear to be always feasible as the ions often exist as complexes and their reduction potential depends on the specific nature of the prevailing complex and its concentration in solution. For the complexes and concentrations used in this study, the approximate electrochemical potentials for reduction have been

Table 1 Reduction potentials for metal ions and metal ion complexes other than Au used in this study (Aylward and Findlay 2002; Bard et al. 1985)

Simple ion	E^o for reduction of simple ion to metal[a]/V vs. SHE[b]	Complex ion	E for reduction of complex at 0.02 M[a]/V vs. SHE
Pt^{2+}	1.18	$PtCl_4^{2-}$	0.76
Pd^{2+}	0.92	Pd^{2+}	0.92
Rh^{3+}	0.7	$RhCl_6^{3-}$	0.5
Ir^{4+}	–[c]	$IrCl_6^{4-}$	0.86
Ru^{3+}	0.68	–	–

[a] E^o, the reduction potential under standard conditions; E, the reduction potential under the conditions prevailing. [b]*SHE*, standard hydrogen electrode. [c]Not known or not determined

estimated (Table 1). All of these are above the 0 V, the estimated reduction potential in vascular plants (Haverkamp and Marshall 2009). It might, therefore, be possible to find treatment protocols that permit particles of the other noble metals to be formed in *C. vulgaris* or other algae.

Conclusions

Live *C. vulgaris* cells exposed to gold salts produced copious quantities of gold nanoparticles in the cytoplasm as observed by TEM and characterized by XRD and XAS. Levels of 1.4% Au were obtained with better than 97% recovery efficiency. In view its ease of cultivation and the ability to form large amounts of intracellular nanogold, combined with its ease of cultivation, rapid growth, and ease of disruption to release intracellular contents, *C. vulgaris* provides a potentially attractive route to commercial production of gold nanoparticles. *C. vulgaris* appeared to be less effective in reducing the other noble metal salts to crystalline metals.

Acknowledgments Jianyu Chen, Manawatu Microscopy Centre, Palmerston North, Massey University, New Zealand, assisted with the TEM study. Some of the measurements were made at the Australian Synchrotron, Melbourne, Australia. Travel funds were provided by the New Zealand Synchrotron Group Ltd. Melissa Basil-Jones and Katie Sizeland assisted with the synchrotron data collection.

References

Andersen RA (ed) (2005) Algal culturing techniques. Elsevier, Burlington

Anderson CWN, Brooks RR, Stewart RB, Simcock R (1998) Harvesting a crop of gold in plants. Nature 395:553–554

Aylward G, Findlay T (2002) SI chemical data, 5th edn. Wiley, Milton

Bard AJ, Parsons R, Jordan J (1985) Standard potentials in aqueous solution. Marcel Dekker, New York

Brayner R, Barberousse H, Hernadi M, Djedjat C, Yepremian C, Coradin T et al (2007) Cyanobacteria as bioreactors for the synthesis of Au, Ag, Pd, and Pt nanoparticles via an enzyme-mediated route. J Nanosci Nanotechnol 7: 2696–2708

Chisti Y (2007) Biodiesel from microalgae. Biotechnol Adv 25:294–306

Chisti Y (2008) Biodiesel from microalgae beats bioethanol. Trends Biotechnol 26:126–131

Chisti Y (2010) Fuels from microalgae. Biofuels 1:233–235

Chisti Y, Moo-Young M (1986) Disruption of microbial-cells for intracellular products. Enzyme Microbol Technol 8:194–204

Farrow CL, Juhas P, Liu JW, Bryndin D, Bozin ES, Bloch J et al (2007) PDFfit2 and PDFgui: computer programs for studying nanostructure in crystals. J Phys Condens Matter 19:335219

Gardea-Torresdey J, Parsons J, Gomez E, Peralta-Videa J, Troiani H, Santiago P et al (2002) Formation and growth of Au nanoparticles inside live alfalfa plants. Nano Lett 2:397–401

Haruta M (2003) When gold is not noble: catalysis by nanoparticles. Chem Rec 3:75–87

Haverkamp RG (2010) Ten years of nanoparticle research in Australia and New Zealand. Part Sci Technol 28:1–40

Haverkamp RG, Marshall AT (2009) The mechanism of metal nanoparticle formation in plants: limits on accumulation. J Nanopart Res 11:1453–1463

Haverkamp RG, Wallwork KS (2009) X-ray pair distribution function analysis of nanostructured materials using a Mythen detector. J Synchrotron Radiat 16:849–856

Haverkamp RG, Marshall AT, van Agterveld D (2007) Pick your carats: nanoparticles of gold-silver-copper alloy produced in vivo. J Nanopart Res 9:697–700

Lamb AE, Anderson CWN, Haverkamp RG (2001) The extraction of gold from plants and its applications to phyto-mining. Chem NZ 65:31–33

Manceau A, Nagy KL, Marcus MA, Lanson M, Geoffroy N, Jacquet T et al (2008) Formation of metallic copper nanoparticles at the soil-root interface. Environ Sci Technol 42:1766–1772

Marshall AT, Haverkamp RG, Davies CE, Parsons JG, Gardea-Torresdey JL, van Agterveld D (2007) Accumulation of gold nanoparticles in *Brassica juncea*. Int J Phytorem 9:197–206

Mohanpuria P, Rana NK, Yadav SK (2008) Biosynthesis of nanoparticles: technological concepts and future applications. J Nanopart Res 10:507–517

Molina Grima E, Belarbi E-H, Acién Fernández FG, Robles Medina A, Chisti Y (2003) Recovery of microalgal biomass and metabolites: process options and economics. Biotechnol Adv 20:491–515

Qiu X, Thompson JW, Billinge SJL (2004) PDFgetX2: a GUI-driven program to obtain the pair distribution function from X-ray powder diffraction data. J Appl Cryst 37:678

Reith F, Etschmann B, Grosse C, Moors H, Benotmane MA, Monsieurs P et al (2009) Mechanisms of gold biomineralization in the bacterium *Cupriavidus metallidurans*. Proc Nat Acad Sci USA 106:17757–17762

Sharma NC, Sahi SV, Nath S, Parsons JG, Gardea-Torresdey JL, Pal T (2007) Synthesis of plant-mediated gold nanoparticles and catalytic role of biomatrix-embedded nanomaterials. Environ Sci Technol 41:5137–5142

Suh IK, Ohta H, Waseda Y (1988) High-temperature thermal-expansion of 6 metallic elements measured by dilatation method and X-ray-diffraction. J Mater Sci 23:757–760

Xie JP, Lee JY, Wang DIC, Ting YP (2007) Identification of active biomolecules in the high-yield synthesis of single-crystalline gold nanoplates in algal solutions. Small 3:672–682